THE JOURNAL OF BIOLOGICAL CHEMISTRY
Vol. 271, No. 52, Issue of December 27, pp. 33268–33276, 1996

Printed in U.S.A.

In Vitro Studies of the Prp9·Prp11·Prp21 Complex Indicate a Pathway for U2 Small Nuclear Ribonucleoprotein Activation*

(Received for publication, May 1, 1996, and in revised form, August 12, 1996)

Debra K. Wiest‡, Christine L. O'Day§, and John Abelson¶

From the Division of Biology, California Institute of Technology, Pasadena, California 91125

Pre-mRNA splicing takes place on a large ribonucleoprotein particle, the spliceosome which contains the five small nuclear ribonucleoproteins (snRNPs), U1, U2, U4, U5, and U6. In *Saccharomyces cerevisiae* the mRNA splicing factors, Prp9, Prp11, and Prp21, are necessary for addition of the U2 snRNP to the pre-mRNA in an early step of spliceosome assembly. This paper describes a study of interactions between these proteins and their role in spliceosome assembly. The proteins were expressed in *Escherichia coli.* Prp9 and Prp11 were purified by metal affinity chromatography. Prp21 was purified using a solubilization/renaturation protocol. We have combined these separately purified proteins and present direct evidence of a Prp9·Prp11·Prp21 protein complex that is functional in *in vitro* splicing assays. Characteristics of this Prp9·Prp11·Prp21 complex were further investigated using proteins synthesized *in vitro*. In addition, we found that Prp9, Prp11, and Prp21 influence the structure of the U2 snRNP in a manner that alters the accessibility of the branch point pairing region of the U2 snRNA to oligonucleotide- directed RNaseH cleavage. We present a model, based on the data presented here and in the accompanying paper, for a combined role of Prp9, Prp11, Prp21, and Prp5 in activating the U2 snRNP for assembly into the pre-spliceosome.

Eukaryotic pre-mRNA splicing is a dynamic process involving a complex array of RNA-RNA and RNA-protein interactions (reviewed in Refs. 1 and 2). These interactions take place on a large, multi-protein RNA complex called the spliceosome. Assembly of the spliceosome occurs by ordered association of five snRNPs[1] with the pre-mRNA substrate. Initially, the U1 snRNP associates with the pre-mRNA, followed by the U2 snRNP and finally the U4/U6·U5 tri-snRNP. The two transesterification reactions leading to intron removal and exon ligation are thought to be catalyzed by the RNA components of the spliceosome (reviewed in Ref. 3). The spliceosomal proteins are thought to facilitate modulation and stabilization of RNA structures critical for the splicing reaction.

A large number of proteins required for pre-mRNA splicing have been identified in yeast (4, 5). Some of these proteins can be found stably associated with specific snRNPs. Others are components of spliceosome complexes. Yet another class of splicing proteins acts transiently to facilitate spliceosome formation.

The initial step in spliceosome assembly is the stable association of the U1 snRNP with the pre-mRNA (reviewed in Ref. 2). This step requires sequence elements in the pre-mRNA at the 5′ splice site and the branch point. Pre-spliceosome formation occurs when the U2 snRNP adds to the U1·pre-mRNA complex. U2 binding also requires sequences in the branch point pairing region of the pre-mRNA. These sequences become paired to the complementary branch point region of the U2 snRNA (2). The branch point region of U2 is situated between two highly conserved secondary structural elements (6). One of these is the 5′ stem-loop structure and the other is a set of stem-loops with pseudoknot characteristics (7, 8). U2 cold-sensitive mutations and revertants in this pseudoknot-like region have suggested potential structural transitions that may be important for U2 snRNP activities, including pre-spliceosome formation (9, 10).

Four proteins known to be required for stable association of the U2 snRNP with the pre-mRNA are Prp5, Prp9, Prp11, and Prp21 (reviewed in Ref. 11). Prp5 is a member of the DEAD family of putative RNA helicases (12), and Prp9 and Prp11 contain amino acid homology to the TFIIIA type zinc finger RNA binding domains (13, 14). Prp21 is a member of a family of proteins related in sequence to the *Drosophila* gene, *suppressor of white apricot* (15). The finding that mutant alleles of the *PRP5, PRP9, PRP11,* and *PRP21* genes show synthetic lethal genetic interactions suggested a tightly coupled role for the corresponding proteins in splicing (16, 17). That these proteins also interact genetically with the cold-sensitive U2 mutations described above suggested that changes in the structure of the U2 snRNA may be critical to the activities of Prp5, Prp9, Prp11, and Prp21 (16, 17). Pre-spliceosome formation requires ATP hydrolysis. Because Prp5 is an RNA-dependent ATPase (18), it is tempting to speculate that Prp5 is responsible, at least in part, for the ATP dependence of pre-spliceosome formation. Could such an ATP-dependent reaction by Prp5 be coupled to U2 snRNA structural changes and the activity of Prp9, Prp11, and Prp21? To better understand these genetic interactions, we have purified the Prp9, Prp11, and Prp21 proteins using recombinant *Escherichia coli* expression systems. Purification of these proteins has allowed us to investigate their biochemical characteristics and their interactions with Prp5 and the U2 snRNP.

MATERIALS AND METHODS

Plasmid Construction—The following oligonucleotides were used in the cloning manipulations described below: 1) 5′CATCATCTCCATGGATTTACTTG; 2) 5′CAGAGGATCCTCACACCAAACC; 3) 5′CCTCGACCATGGACTTGTCGTCGTCGTCGAT; 4) T7 promoter sequencing primer; 5) 5′CATAGAATTCATATGAACTATTTAGAAG; 6) 5′CAAGAATTCGGATCCTACTGTCATACATC.

* The research was supported by Grant GM32637 from the National Institutes of Health. The costs of publication of this article were defrayed in part by the payment of page charges. This article must therefore be hereby marked "*advertisement*" in accordance with 18 U.S.C. Section 1734 solely to indicate this fact.

‡ Supported by a grant from the Jane Coffin Childs Memorial Fund for Medical Research. Present address: Hewlett-Packard Co., Palo Alto, CA.

§ Present address: Oridigm Corp., Seattle, WA.

¶ To whom correspondence should be addressed. Tel.: 818-395-3945; Fax: 818-796-7066; E-mail: abelsonj@starbase1.caltech.edu.

[1] The abbreviations used are: snRNP, small nuclear ribonucleoprotein; PCR, polymerase chain reaction; PAS, protein A-Sepharose; PAGE, polyacrylamide gel electrophoresis.

Several Prp9, Prp11, and Prp21 *E. coli* expression vectors were constructed and used in these experiments. To construct the plasmid pET-Prp9, the Prp9 coding region of the plasmid pPrp9–3′HA (kindly provided by M. Rosbash, Brandeis University) was amplified by the polymerase chain reaction (PCR) with oligonucleotides 1 and 2 described above. This generated *Nco*I and *Bam*HI restriction site at the 5′ and 3′ ends, respectively. The resulting fragment was digested with *Nco*I and *Bam*HI and ligated into pET16b (Novagen, Inc., Madison, WI) restricted with the same enzymes. The normal amino acid at position 2 of Prp9 is Asn. However, due to the conversion of the sequence at this position to an *Nco*I site the amino acid at the second position was changed to Asp. The dideoxy chain termination DNA sequencing method was used to verify the sequence of the Prp9 insert. To construct the His-tagged Prp9 expression vector the His-tag region from pET19b (Novagen) was PCR-amplified with primers 3 and 4 described above. The downstream primer generated an *Nco*I site just after the His-tag region. The resulting PCR fragment was digested with *Nco*I, and the His-tag fragment was ligated into pET-Prp9 (described above). Protein expressed from this plasmid has the following amino-terminal sequence: $M(H)_{10}$SSGHIDDDDKS–MD. The penultimate Met immediately following the dash corresponds to the original Met of Prp9. The Asp at the normal second position is changed from an Asn as described above.

To construct the plasmid pET-HisPrp11, the coding region of Prp11 was amplified from the plasmid pPrp11-cen (16). Sequences for *Nde*I and *Bam*HI were included in the amplifying primers. The resulting PCR fragment was digested with *Nde*I and *Bam*HI and ligated into pET19b restricted with the same enzymes. Protein expressed from this plasmid contains the following amino-terminal sequence: $M(H)_{10}$SSGHIDDDDKS–MN. The two amino acids following the dash represent the first two amino acids of the Prp11 coding region. The DNA sequence of the Prp11 insert was verified by sequencing as described above. To construct the plasmid pET-Prp11, pET-HisPrp11 was digested with *Nde*I and *Bam*HI, and the resulting Prp11 fragment was isolated. This fragment was ligated into pET11a (Novagen) restricted with *Nde*I and *Bam*HI. The Prp21 expression plasmid pET-Prp21, was described previously (19). To construct pET-HisPrp21 the *Nde*I fragment from pET-Prp21 containing Prp21 DNA sequences was ligated into the *Nde*I site of pET-19b. DNA sequencing as described above was used to verify the correct orientation of the insert.

Protein Purification—Expression and purification of His-Prp9 was performed in the *E. coli* strain HMS-pLysS. Expression levels for His-Prp9 in this strain were slightly better than in BL21, albeit still extremely low. To purify Prp9, competent *E. coli* cultures were freshly transformed. Cells were used within 24 h of transformation to inoculate an overnight culture. The following day, 3 liters of broth was inoculated with 5 ml of the saturated overnight culture. The culture was grown to an A_{600} of 0.6, at which time isopropyl-D-thiogalactopyranoside was added to a final concentration of 0.8 mM. After 3½ h of growth at 37 °C, cells were harvested by centrifugation at 5000 × *g*. From this point all manipulations were performed at 4 °C. Pelleted cells were resuspended in 95 ml of buffer IMAC5 (20 mM Tris-HCl, pH 7.5, at room temperature, 0.5 M NaCl, 10% glycerol, 5 mM imidazole) + 1 mM phenylmethylsulfonyl fluoride. Cells were lysed on ice by four repeated rounds of a 30-s sonication followed by a 30-s rest. The lysate was cleared by centrifugation and the supernatant was recovered. The lysate was diluted to ≤10 mg/ml protein and loaded onto a 2-ml Ni-NTA (Quiagen) column equilibrated in IMAC5. The column was washed with 40 ml of IMAC5 followed by 20 ml of IMAC25 (same as above except 25 mM imidazole). His-Prp9 was stepped off the column with IMAC200 (same as above except 200 mM imidazole). Protein-containing fractions were pooled and dialyzed against P9 buffer (20 mM Tris-HCl, pH 7.9, at 4 °C, 100 mM KCl, 0.2 mM EDTA, 20% glycerol). Protein was stored frozen at −70 °C at a concentration of 2 mg/ml. His-Prp9 purified in this manner was 40–50% pure as determined by SDS-PAGE and staining with Coomassie Blue. The majority of contaminating protein was represented by a single band at 25–30 kDa.

Expression and purification of His-Prp11 was performed in the *E. coli* strain BL21. Transformation, growth, and isopropyl-D-thiogalactopyranoside induction of cells were as described above for His-Prp9, as was cell harvest and lysate preparation except that His-Prp11 containing cells were lysed in buffer containing 100 mM KCl, 20 mM Tris-HCl, pH 7.9, at 4 °C, 0.2 mM EDTA, 20% glycerol, and 1 mM phenylmethylsulfonyl fluoride. His-Prp11 was purified by chromatography on S-Sepharose prior to Ni-affinity chromatography. The cell lysate was loaded onto a 5 ml of S-Sepharose column. The column was washed with the same buffer described above except lacking EDTA. His-Prp11 was stepped off the column in buffer containing 500 mM KCl, 20 mM Tris-HCl, pH 7.9, at 4 °C, and 20% glycerol. Fractions containing protein were pooled, and KCl and imidazole were added to final concentrations of 0.5 M and 5 mM, respectively. The protein was loaded onto a 2 ml Ni-NTA column and chromatographed as described above for His-Prp9. Eluted His-Prp11 was dialyzed against P11 buffer (20 mM Tris-HCl, pH 7.9, at 4 °C, 20% glycerol, 0.2 mM EDTA, 1 mM $ZnCl_2$, and 0.5 M KCl). Protein was stored at −70 °C at a concentration of 0.2 mg/ml. His-Prp11 purified in this manner was >90% pure as determined by SDS-PAGE and silver staining.

Prp21 was purified in BL21 from inclusion bodies. Transformation, isopropyl-D-thiogalactopyranoside induction, and cell lysis were as described above. After centrifugation of the lysate, the inclusion body pellet was recovered and transferred to a chilled glass beaker. Solubilization buffer (10 mM HEPES, pH 7.9, 6 M guanidine HCl, 0.2 mM EDTA, 0.2 mM EGTA, and 10 mM dithiothreitol) was added, and the mixture was stirred gently for 8 h at 4 °C. Cellular debris was removed by centrifugation at 18,000 rpm in an SS34 rotor. The supernatant was diluted to 1 M guanidine with solubilization buffer lacking guanidine. The sample was then dialyzed against 20 mM HEPES, pH 7.9, 20% glycerol, 0.1 M KCl, 0.2 mM EDTA, 0.2 mM EGTA, and 2 mM dithiothreitol. Prp21 protein was stored at −70 °C at a final concentration of 0.2 mg/ml. Prp21 protein purified in this manner was ≥90% pure as determined by silver staining of SDS-PAGE. For some experiments described below, Prp21 protein purified in the above manner was added to purified His-Prp11, and the combination was repurified on Ni-NTA. This chromatography step resulted in recovery of equimolar amounts of His-Prp11 and Prp21 when excess Prp21 was present in the mixture.

In Vitro Translation and His-tagged Protein Binding Assays—mRNAs for tagged and untagged Prp9, Prp11, and Prp21 were synthesized *in vitro* with T7 RNA polymerase from the above expression vectors restricted with *Hin*dIII. mRNA was purified by phenol/$CHCl_3$ extraction and ethanol precipitation. *In vitro* translation reactions were performed with a rabbit reticulocyte kit (Promega). Reactions were performed as per manufacturer's instructions. Briefly, a mixture consisting of reticulocyte, RNase inhibitor, amino acids minus methionine, and [^{35}S]methionine (DuPont NEN) was added to a specific mRNA that had been preheated at 65 °C in H_2O. The amount of mRNA for each Prp synthesis required for maximum yield of translation product was empirically determined in test reactions. This amount varied for different Prp mRNAs. Reactions were incubated for 60 min at 30 °C. Samples subjected to SDS-PAGE analysis were precipitated with four volumes of acetone at 20 °C for ≥30 min. Recovered pellets were resuspended in SDS buffer and loaded on an SDS-PAGE gel. ^{35}S-Labeled products were visualized by autoradiography.

Protein-protein binding assays were performed with *in vitro* translation products consisting of one His-tagged protein and one or more non-tagged proteins. For most assays, ^{35}S-labeled proteins were combined immediately after synthesis at 30 °C. The mixture was incubated for 20 min at 30 °C and then added to 300 μl of IMAC5 containing 10–15 μl of Ni-NTA beads (Quiagen resin). This mixture was incubated on a rotator at 4 °C for 1 h. Beads were pelleted and the supernatant was recovered. Beads were then washed three consecutive times with 1 ml of IMAC5. Beads were then resuspended in 300 μl of IMAC25 and incubated 20 min. Beads were pelleted; the supernatant was recovered, and beads were again washed in IMAC25 as described above. The procedure was repeated with IMAC50. Finally, beads were resuspended in 300 μl of IMAC200, incubated for 20 min, and the supernatant from this final incubation was recovered. Each supernatant described above was precipitated with four volumes of acetone and the pellets were subjected to SDS-PAGE as described above.

Yeast Extract Preparation and in Vitro Splicing Assays—Yeast extracts from the temperature-sensitive strains *prp9-1*, *prp11-1*, and *prp21-1* were prepared as described previously (20). Mutant extracts were inactivated by incubation at 37 °C for 25–30 min, except for the *prp21-1* extract which was heat-inactivated by incubation at 39 °C for 7–8 min. Splicing assays using a synthetic yeast actin pre-mRNA substrate were as described previously (20). Splicing assays with heat-inactivated mutant extracts reconstituted with purified protein were generally performed by addition of protein to the heat-treated extracts, followed by addition of splicing buffer and actin pre-mRNA substrate to initiate the reaction. In the experiment of Fig. 2, some reactions were performed by addition of purified protein to the mutant extract prior to heat treatment, as indicated in the legend. The amount of purified protein required to reconstitute splicing activity in heat-treated *prp9-1*, *prp11-1*, and *prp21-1* extracts was typically 1–10 nM. It is difficult to estimate endogenous levels of these proteins in normal yeast extracts because our antibodies do not detect Prp9, Prp11, or Prp21 in Western blots of crude extracts. However, if the concentration of these proteins

is comparable to the concentrations of snRNPs in active extracts (5 nM) then the recombinant proteins are quite active.

RNaseH Structure Probing—RNaseH digestion of U2 snRNA in mutant extracts and analysis of cleaved U2 snRNA were performed as described in the accompanying paper (18).

snRNA Reconstitution and Immunoprecipitation—The protocols for knock out and reconstitution of endogenous U6 and U2 snRNA in wild type yeast extracts described by Fabrizio *et al.* (21) and McPheeters *et al.* (22) were used to reconstitute extracts with synthetic radiolabeled U2 and U6 snRNAs. Briefly, wild type yeast extract was incubated with either the d1 oligo (140 nM final concentration) for U6 knockout or the SRU2 oligo (200 nM final concentration) for U2 knockout under splicing reaction conditions (60 mM phosphate, 3 mM $MgCl_2$, 6 mM ATP, 3% polyethylene glycol, 1.2 mM spermidine, and 10 mM dithiothreitol) for 30 min at 30 °C. Synthetic U2 snRNA or U6 snRNA, labeled by transcription in reaction mixtures containing [α-^{32}P]UTP, was then added followed by H_2O or actin pre-mRNA splicing substrate. Reactions were incubated for 15–20 min at room temperature and then added to an equal volume of antibody attached to protein A-Sepharose beads (PAS). Antibody attached to PAS was prepared as described by Arenas and Abelson (19). Mixtures were incubated for 30 min on ice with frequent mixing of the components. Beads were pelleted and washed three times in NET2 buffer (40 mM Tris-HCl, pH 7.5, at room temperature, 150 mM NaCl, 0.05% Triton). Beads were then proteinase K-treated and processed as described previously for splicing reactions (20). Recovered RNA was analyzed by denaturing gel electrophoresis. Immunodepletion of spliceosomal complexes by Prp21 antibodies was performed as described by Arenas and Abelson (19). For immunodepletion of reactions performed in *prp2-1* mutant extracts, the extract was heat-inactivated for 30 min at 37 °C prior to reaction with actin pre-mRNA substrate.

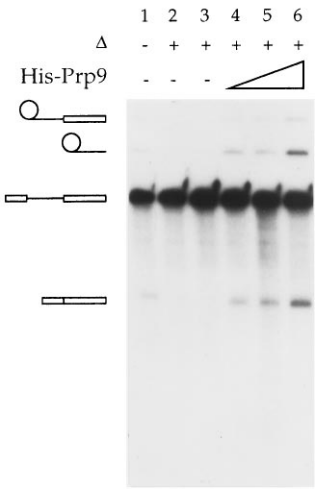

FIG. 1. **Reconstitution of splicing activity in *prp9-1* mutant extracts with purified Prp9 protein.** Splicing assays with an actin pre-mRNA substrate were performed as described under "Materials and Methods" with 4 liters of extract from the *prp9-1* strain in a total reaction volume of 10 μl. Reactions were for 50 min at 15 °C. In the reactions of *lane 1*, the *prp9-1* extract did not receive heat treatment, whereas in *lanes 2–6* the extract was heated at 37 °C for 30 min (indicated by Δ). For the reactions in *lanes 3–6*, increasing concentrations of His-Prp9 protein were added and constituted 1/10 of the total reaction volume. In reactions where His-Prp9 protein was not added, H_2O (*lanes 1* and *2*) or buffer (*lane 3*) was added instead.

RESULTS

Purification of Prp9, Prp11, and Prp21 Proteins—To begin to investigate the mechanism of action of Prp9, Prp11, and Prp21 in pre-mRNA splicing, we have purified the three proteins using bacterial expression systems. Purification of Prp9 and Prp11 was facilitated through the use of amino-terminal, nickel affinity tags and IMAC as described under "Materials and Methods." Expression of Prp21 in *E. coli* leads to production of highly insoluble material (19); therefore, a strategy for solubilization and renaturation of Prp21 from inclusion bodies was designed and is described under "Materials and Methods."

Each of our purified proteins was tested in *in vitro* splicing assays for the ability to restore splicing activity to the corresponding mutant yeast extract. As shown in Fig. 1 heat inactivation and reconstitution of extracts from the *prp9-1* mutant strain with purified Prp9 protein were efficient (*lanes 4–6*) with reconstitution giving splicing levels similar to that of wild type extracts. Reconstitution of splicing activity of extracts from the *prp11-1* or *prp21-1* mutant strains was consistently less efficient. It was previously noted by Chang *et al.* (14) that reconstitution of *prp11-1* extracts with *in vitro* translated Prp11 protein required addition of the protein to the extract prior to heat treatment. We therefore tested this protocol with our purified Prp11 and Prp21 proteins. In the experiment of Fig. 2, Prp11 protein was added either before or after heat treatment of a *prp11-1* mutant extract. Addition of Prp11 protein restored splicing to a significant level only when added before heat treatment (compare *lanes 3* and *4*). The observation that heat treatment of the *prp11-1* mutant extract resulted in permanent inactivation of the extract led Chang *et al.* (14) to propose that Prp11 may be an integral part of a complex whose components were also inactivated upon heat treatment of the mutant extract. To test the possibility that a Prp9, Prp11, Prp21 complex was inactivated in these heat treatments, we assayed for reconstitution of splicing when combinations of Prp9, Prp11, and Prp21 protein were added either before or after heat inactivation of the *prp11-1* mutant extract. The ability to reconstitute splicing by proteins added after heat treatment could only be detected when all three proteins were added (*lane 8*). This finding indicates that heat treatment of extracts containing the *prp11-1* allele also leads to inactivation of Prp9 and Prp21. Experiments performed with the three purified proteins and the *prp21-1* mutant extract showed similar results, indicating that heat treatment of extracts containing the *prp21-1* allele leads to inactivation of Prp9 and Prp11 in addition to Prp21 (*lanes 11–18*).

Prp9·Prp11·Prp21 Complex Formation in Vitro—In an attempt to characterize the putative Prp9·Prp·11·Prp21 complex, we investigated other methods to obtain the three proteins in active form. We synthesized these proteins *in vitro* utilizing a rabbit reticulocyte lysate for translation of synthetic mRNAs corresponding to each of the three proteins. The polypeptides were synthesized with [^{35}S]methionine, and, as shown in Fig. 3*A*, each translation product has the predicted molecular weight. Each of these *in vitro* translated proteins reconstitutes splicing activity in the corresponding heat-treated mutant extract (data not shown).

Several previous experiments suggested that Prp9, Prp11, and Prp21 formed a complex *in vivo* (16, 23, 24). To test for complex formation in the absence of other yeast proteins or snRNA's, we utilized our nickel affinity-tagged constructs to test for protein-protein interaction based on co-purification of untagged with tagged protein. The protocol for the binding experiment is diagrammed in Fig. 3*B*. *In vitro* translated proteins were prepared in separate translation reactions. The reactions were combined, incubated briefly, and added to Ni-NTA resin in buffer containing 5 mM imidazole. The mixture was then spun to pellet the beads and the supernatant removed. Beads were washed repeatedly in this fashion in 5 mM Imidazole buffer. Buffer containing increasing concentrations of Imidazole was then used to successively wash the beads, and the supernatants were analyzed by SDS-PAGE. Results of an experiment with His-tagged Prp11 and untagged Prp9 and Prp21 are shown in Fig. 3*C*. In the experiment of *lanes 1–5*, reactions were combined such that the His-Prp11 protein was present at a reduced molar ratio relative to the untagged proteins. When a mixture of tagged Prp11 and untagged Prp9 and Prp21 were added to the beads, both Prp21 and Prp9 co-bound with tagged Prp11, as illustrated by their presence in the 55

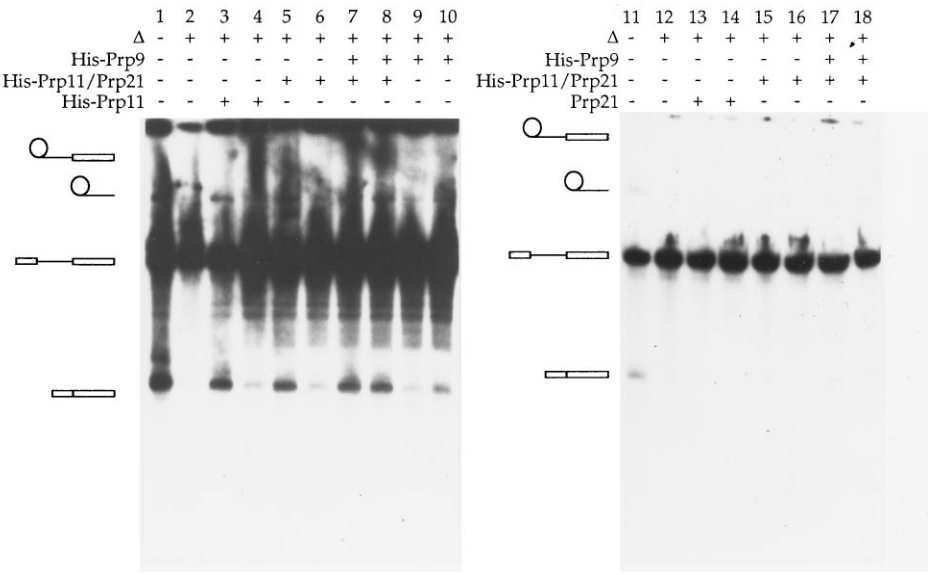

FIG. 2. **Reconstitution of splicing activity in *prp11-1* and *prp21-1* mutant extracts with purified Prp9·Prp11·Prp21 complex.** Splicing assays as described in the legend of Fig. 1 were performed with extracts from the *prp11-1* mutant strain (*lanes 1–10*) and with extracts from the *prp21-1* mutant strain (*lanes 11–18*). In the reactions of *lanes 2–18*, mutant extracts were heated in the absence (*even numbered lanes*) or presence (*odd numbered lanes*) of added purified protein. For the reactions heat-treated in the absence of added purified protein, the indicated proteins were added after heat treatment (except *lanes 2* and *12*) and before initiation of the splicing reaction by addition of splicing buffer and actin pre-mRNA. The combination of proteins added to each reaction is indicated *above* the lane. Heat treatment of mutant extracts was for 25 min at 37 °C (*prp11-1* mutant extracts, *lanes 2–10*) or for 8 min at 39 °C (*prp21-1* mutant extracts, *lanes 12–18*). In reactions containing the two proteins His-Prp11 and Prp21 (*lanes 5–8* and *15–18*), the source of protein was His-Prp11 and Prp21 co-purified on Ni-NTA as described under "Materials and Methods." In reactions to which all three Prps were added (*lanes 7, 8, 17,* and *18*), the purified proteins were mixed at the appropriate dilution prior to addition to the heat-treated extract.

and 200 mM Imidazole washes (*lanes 3* and *4*). Control experiments in which the His-tagged protein was omitted from the binding reaction and only Prp9 and Prp21 were incubated with the beads resulted in elution of both proteins in the 5 mM Imidazole supernatant (*lane 11*). The elution profile of His-Prp11 alone is similar to that observed when Prp9 and Prp21 are present (*lanes 6-10*). The specific activity of each of the *in vitro* translated proteins was determined, and the amount of each protein in the 55 and 200 mM Imidazole elutions was measured as described under "Materials and Methods." In the elutions of *lanes 3* and *4*, equimolar amounts of Prp11 and Prp21 were obtained. A 3–4-fold lower amount of Prp9 was observed in these lanes. The experiment of Fig. 3*C* was repeated multiple times, varying the relative molar ratios of the tagged to untagged proteins. In all experiments where the input amount of Prp21 relative to His-tagged Prp11 was one or greater, the recovered molar ratio of Prp11 to Prp21 was 1. We had difficulty producing large quantities of Prp9 *in vitro* and were therefore unable to load a large excess of Prp9 relative to Prp11; thus the relative molar ratio of Prp9 to Prp11 in these experiments was consistently at or below 1.

The His-tag/Ni-binding experiments described above were also performed with combinations of Prp9·Prp11·Prp21 in which either Prp9 or Prp21 contained the His-tag. The *in vitro* synthesized Prp21 and Prp9 with amino-terminal His-tags were first tested to ensure their activity in reconstitution of splicing in mutant yeast extracts (data not shown). Table I summarizes the results of the binding assays. Also included is a summary of the results from the binding studies in Fig. 3*C*. In pairwise experiments we consistently observed co-elution of Prp11 and Prp21, Prp9 and Prp21, and Prp21 with both Prp11 and Prp9. In experiments which tested for co-elution of two untagged proteins with one tagged protein, we consistently observed co-elution of the two untagged proteins, regardless of which protein was tagged. Taken together, these results are most consistent with a model for the Prp9·Prp11·Prp21 complex in which the interactions are contributed for the most part in highly stable pairwise interactions of Prp9 with Prp21 and Prp11 with Prp21. In addition, quantitation of the molar ratios of proteins in the pairwise combinations and in the three protein experiments described above strongly support there being equimolar amounts of Prp9, Prp11, and Prp21 in the complex (data not shown).

Functional Interaction between Prp5 and Prp9·Prp11·Prp21—There are several lines of evidence suggesting that Prp5 may interact with Prp9, Prp11, and Prp21. First, the four proteins are required at the same step in spliceosome assembly, namely the stable addition of U2 snRNP to the pre-mRNA (2, 11). Second, combinations of pairs of the temperature-sensitive alleles of Prp5, Prp9, Prp11, and Prp21 show a synthetic lethal phenotype *in vivo* (16, 17). The most likely mechanism for the observed synthetic lethality between Prp9, Prp11, and Prp21 is the inactivation of the Prp9·Prp11·Prp21 complex. It is possible that a similar interaction explains the genetic interaction between Prp5 and Prp9, Prp11, or Prp21. We therefore tested for a direct interaction between Prp5 and the Prp9·Prp11·Prp21 complex using the His-tag/nickel binding experiment described above. Under all conditions tested we were unable to detect significant binding of Prp5 to Prp9·Prp11·Prp21 (data not shown). Prp5 synthesized *in vitro* was active in reconstitution of splicing activity in *prp5-1* mutant yeast extracts (data not shown). This was also the case for binding assays performed in the presence of a molar excess of synthetic U2 snRNA or pre-mRNA (data not shown). Our inability to detect a stable interaction between Prp5 and Prp9·Prp11·Prp21 suggests that the genetic interactions between Prp5, Prp9, Prp11, and Prp21 may be mediated through a functional rather than a physical interaction between these proteins, *i.e.* the four proteins may be acting on the same substrate.

Several lines of evidence suggest that Prp9, Prp11, Prp21, and Prp5 act in conjunction with the U2 snRNP (16, 17). In the accompanying paper (18) we employ an RNaseH structure probing assay to show that Prp5 plays a role in an ATP-mediated structural change of the U2 snRNP. In the experi-

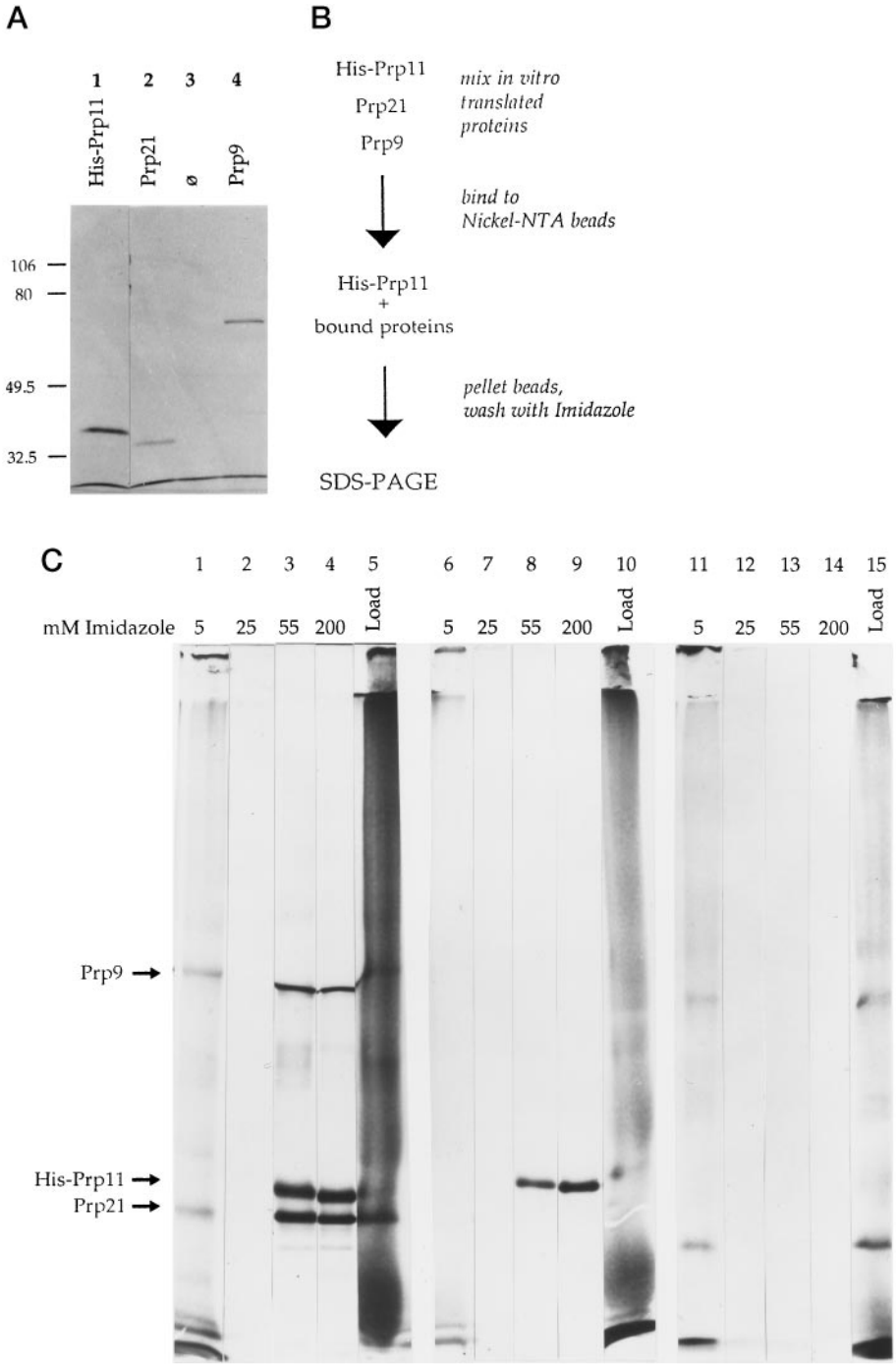

FIG. 3. **Prp9·Prp11·Prp21 complex formation *in vitro*.** *A*, ^{35}S-labeled proteins were synthesized by *in vitro* translation as described under "Materials and Methods." An aliquot of the reaction was acetone-precipitated, processed, and analyzed by SDS-PAGE. An autoradiogram from the gel is shown. The specific mRNA used in the translation reaction is indicated above each lane. *B* shows a diagram of the protein binding experimental protocol. Binding reactions were performed as detailed under "Materials and Methods." *C*, equal amounts of supernatants recovered by successive elutions from beads with increasing concentrations of Imidazole were processed and analyzed on an 8% SDS-PAGE. An autoradiogram of the gel is shown. The concentration of Imidazole corresponding to the elution sample is indicated *above* each lane. Lanes labeled *Load* represent an aliquot of the protein mixture prior to addition to the Ni-NTA beads. *Lanes 1–5* show binding reactions performed with combined translation products from reactions with His-Prp11, Prp9, and Prp21 mRNAs. *Lanes 6–10* and *11–15* show elutions from binding reactions performed with products from translation reactions with His-Prp11 mRNA only and with Prp9 and Prp21 mRNAs, respectively.

ments shown in Fig. 4*A* we tested the importance of Prp9, Prp11, and Prp21 in this Prp5-mediated conformational change in the U2 snRNP. The extent of cleavage of the U2 snRNP upon addition of a deoxy oligonucleotide complementary to the branch point pairing region of the U2 snRNA was measured in wild type and *prp9-1* extracts. Incubation of heat-treated wild type extracts with the branch point oligonucleotide shows normal levels of U2 cleavage (Fig. 4*A*, *lane 2*). The level of cleavage in the wild type extract is enhanced upon addition of ATP (*lane 3*). In heat-inactivated *prp9-1* extracts cleavage of U2 occurs independently of the presence of ATP (*lanes 5* and *6*). As shown in *lanes 7* and *8*, when purified Prp9 protein is added to the heat-treated *prp9-1* extract, oligonucleotide-directed cleavage again shows an enhancement upon addition of ATP. We also performed RNaseH structure probing experiments with extracts from *prp11-1* and *prp21-1* mutant strains. As with the *prp9-1* mutant strain, heat-inactivated *prp11-1* and *prp21-1* extracts exhibit a high level of branch point oligonucleotide-directed cleavage of U2 RNA in the presence or absence of ATP. However, when cleavage is monitored in *prp11-1* and *prp21-1* mutant extracts to which the appropriate purified protein has been added, we still observe a high level of cleavage even in the absence of added ATP (data not shown). We believe the latter observation is related to the fact that heat inactivation of mutant extracts of these two alleles can cause irreversible inactivation of splicing activity. Even though in the experiments described above we added the purified proteins prior to heat treatment, restoration of activity is still minimal (see Fig. 2). These structure probing experiments indicate that inactivation of Prp9·Prp11·Prp21 favors formation of a U2 snRNP conformation that is not sensitive to the action of Prp5 and ATP. Although the branch point region in this U2 snRNP

TABLE I
Prp9, Prp11, and Prp21 protein-protein interactions in vitro

His-tagged protein	Test proteins	Co-elution from Ni-Beads
Prp11	Prp9	No
	Prp21	Yes
	Prp11[a]	No
	Prp9 and Prp21	Yes[b]
Prp9	Prp11	ND[c]
	Prp21	Yes
	Prp9[a]	No
	Prp11 and Prp21	Yes[b]
Prp21	Prp9	ND[c]
	Prp11	Yes
	Prp9 and Prp11	Yes[b]

[a] Tagged and untagged proteins were synthesized in the same translation reaction prior to the binding test.
[b] Indicates both test proteins co-elute.
[c] ND, not determined.

conformation is open and accessible to cleavage, the snRNP is not functional because of the absence of Prp9, Prp11, and Prp21. In the presence of Prp9, Prp11, and Prp21, the U2 snRNP conformation becomes inaccessible to cleavage and can only be "opened" by the action of Prp5 and ATP.

To further investigate the importance of the U2 snRNP structural changes described above, we applied the RNaseH structure probing technique to extracts of the two cold-sensitive U2 snRNA mutants G53A and C62U (9, 10). Both of these point mutations exhibit a synthetic lethal phenotype with the temperature-sensitive mutants *prp5-1*, *prp9-1*, *prp11-1*, and *prp21-1* described above (16, 17). Extracts from these two mutant U2 strains are active at a low level in *in vitro* splicing reactions performed at 30 °C but not at 15 °C. When extracts from the G53A and C62U strains were tested with the branch point oligonucleotide for RNaseH degradation at 30 °C, we observed the same level of cleavage in the presence or absence of ATP (see Fig. 4*B*). We attempted to perform the RNaseH degradation experiments at the nonpermissive temperature of 15 °C; however, RNaseH activity could not be observed at this temperature even in wild type extracts (data not shown). Thus, the U2 snRNP conformation in these U2 mutants is similar to that of U2 snRNP formed in the absence of Prp9, Prp11, and Prp21 in that branch point region is accessible to cleavage in the absence of ATP.

Prp21 and Prp11 Are in a U6-containing Spliceosomal Complex—Prp9, Prp11, and Prp21 are known to be required for formation of the pre-spliceosome, a complex containing only the U1 and U2 snRNAs (2, 11). In addition, each of the three proteins has been shown to be a component of the pre-spliceosome. The mammalian counterparts to Prp9, Prp11, and Prp21 (SAP61, SAP62, and SAP114) have been found associated with spliceosomal complexes more mature than the pre-spliceosome (25, 26). In early experiments designed to identify spliceosomal complexes containing Prp21, we used an antibody depletion experiment to show that Prp21 was an integral component of the pre-spliceosome (19). However Prp21 did not appear to be present at later stages of assembly because complexes A2-1, A1, and A2-2 were not depleted. We therefore devised a highly sensitive co-immunoprecipitation assay to test for the presence of Prp21 and Prp11 in more mature spliceosomal complexes that contain U6. Our assay makes use of the knockout/reconstitution protocol for the U6 snRNA developed by Fabrizio *et al.* (21). Using wild type extracts, we depleted endogenous U6 snRNA by incubation with the d1 oligonucleotide. We then reconstituted the extract with a radiolabeled, *in vitro* synthesized, U6 transcript and performed immunoprecipitations with antibodies to either Prp21 or Prp11. Precipitated fractions were analyzed on a denaturing gel to determine the extent of U6

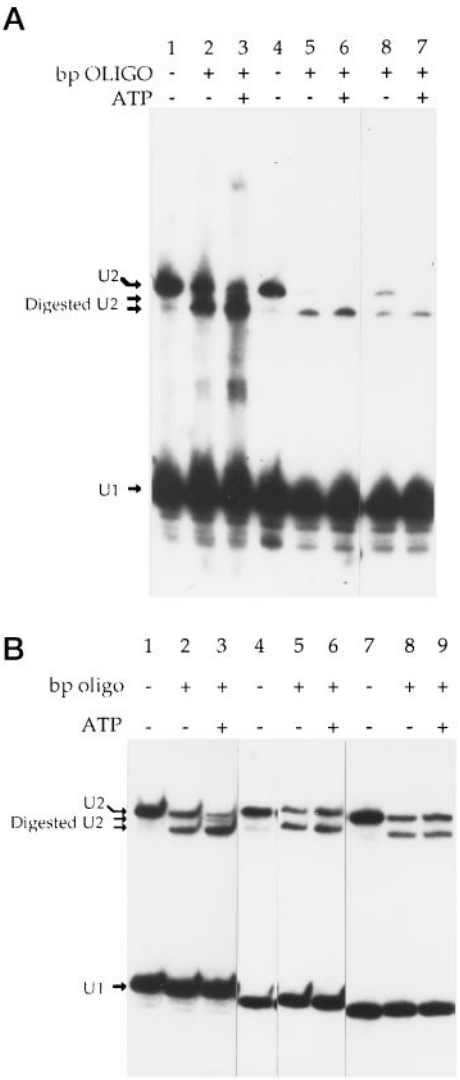

FIG. 4. **RNaseH structure probing of the U2 snRNP in Prp9 and U2 mutant extracts.** *A*, wild type (*lanes 1–3*) or heat-inactivated *prp9-1* mutant extracts (*lanes 4–7*) were incubated with SRU2 oligo (*bp oligo*), *lanes 2, 3* and *5–8*) or H_2O (*lanes 1* and *4*) in the presence or absence of 3 mM ATP as indicated *above* each lane. In the reactions of *lanes 7* and *8*, purified His-Prp9 protein was added to the extract after heat treatment and prior to oligo addition. After oligo treatment at 30 °C for 30 min, reactions were processed, and the U2 snRNA was analyzed by Northern blot hybridization as described under "Materials and Methods." Uncleaved (*i.e.* full length) U2 snRNA is indicated by the *uppermost arrow* labeled *U2*. RNaseH cleaved U2 is indicated by the *two arrows* labeled *Digested U2*. Probes for U1 snRNA were also included in the hybridization as a standard for the amount of RNA sample loaded. *B*, similar experiments as described above in *A*, except extracts were wild type (*lanes 1–3*), mutant U2G53A (*lanes 4–6*), and mutant U2C62U (*lanes 7–9*). *bp*, base pair.

RNA co-precipitation. As shown in Fig. 5, synthetic U6 snRNA co-immunoprecipitates with antibodies to Prp21 and Prp11, in the presence but not the absence of added actin pre-mRNA (compare *lanes 3-6* and *9-12*). This pre-mRNA-mediated U6 co-immunoprecipitation is dependent on a functional 5′ splice site in the actin pre-mRNA (data not shown). In addition, U6 is not co-immunoprecipitated in the absence of ATP, even when wild type pre-mRNA is added (data not shown).

Immunoprecipitations performed with the pre-immune serum for Prp21 showed levels of U6 binding at or below the level seen with the Prp21 antibodies in the absence of added pre-mRNA (data not shown). In other lanes of the experiment of Fig. 5, we depleted wild type extracts of endogenous U2 snRNA by oligonucleotide-directed RNaseH cleavage and re-

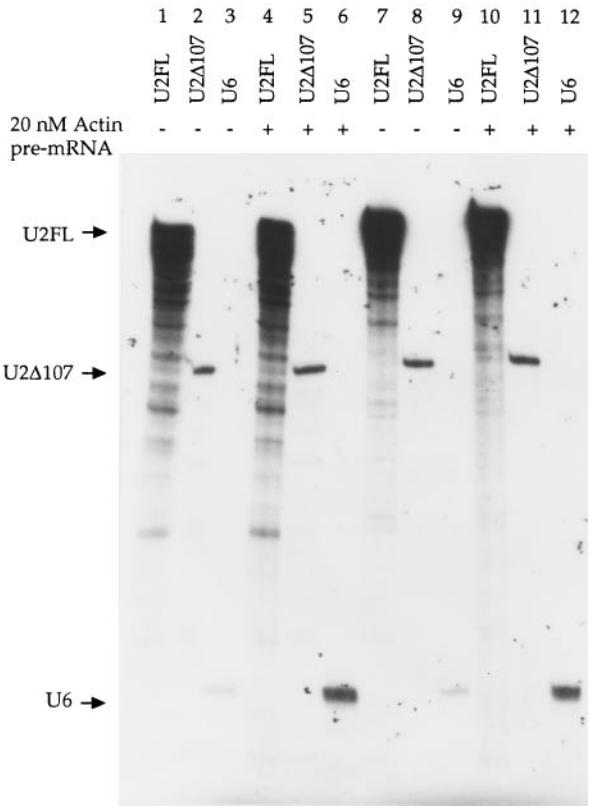

FIG. 5. **Immunoprecipitation of U6 snRNA by Prp11 and Prp21 antibodies.** Wild type yeast extracts were treated with either the SRU2 oligo (U2 knock-out, *lanes 1, 2, 4, 5, 7, 8, 10, 11*) or the d1 oligo (U6 knock-out, *lanes 3, 6, 9, 12*). *In vitro* synthesized, ^{32}P-labeled U2, U2Δ107, or U6 snRNA was added as indicated *above* each lane. H_2O (*lanes 1–3, 7–9*) or unlabeled actin pre-mRNA substrate (*lanes 4–6, 10–12*) was then added, and the reactions were incubated for 15 min at room temperature. Reactions were then added to PAS beads bound with antibodies to either Prp21 (*lanes 1–6*) or Prp11 (*lanes 7–12*) for 30 min on ice. RNA was recovered, processed, and analyzed as described under "Materials and Methods." In most reactions ≥80,000 cpm of snRNA was added to the reaction with recovery amounts of no more than 5000 cpm.

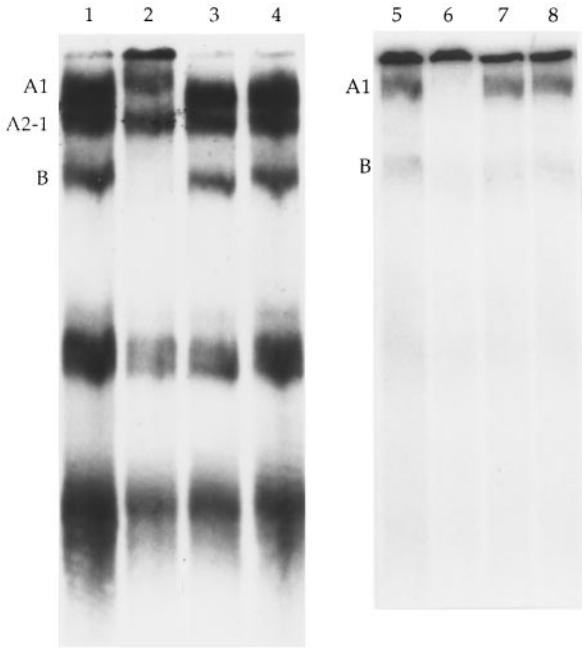

FIG. 6. **Identification of specific spliceosomal complexes containing Prp21.** A standard splicing reaction in a master mix consisting of yeast extract, splicing buffer, and ^{32}P-actin pre-mRNA was incubated for 20 min at room temperature to allow formation of spliceosomes. 15 μl of the reaction was then placed on ice after addition of heparin (12 mg/ml final concentration) and Prp21 antibody PAS beads (5 μl of beads + 5 μl of buffer) and incubated for 30 min. Beads were then pelleted and a portion of the supernatant was loaded on a 3% native gel. An autoradiogram of the gel is shown. *Lanes 1–4* show reactions with wild type yeast extracts performed in the presence of 2 mM EDTA. *Lanes 5–8* show reactions with a heat-inactivated *prp2-1* mutant extract. *Lanes 1* and *5* are control loads of the reaction not treated with PAS. *Lanes 2* and *6* are reactions with Prp21 antibody PAS beads; *lanes 3* and *6* are reactions with PAS beads only, and *lanes 4* and *8* are reactions to which buffer only was added. The position of the pre-spliceosome and the two spliceosomal complexes are indicated by *B*, *A2-1,* and *A1*, respectively.

constituted with a synthetic radiolabeled U2 RNA (22). In this set of experiments we compared the ability of Prp21 and Prp11 antibodies to co-immunoprecipitate a full-length U2 RNA or the internal deletion known as Δ107 (described under "Materials and Methods"). As expected, we observed co-immunoprecipitation of full-length U2 in the presence and absence of added actin pre-mRNA (*lanes 1, 4, 7,* and *10*). This is consistent with earlier antibody precipitation experiments that showed that Prp21 associates with the endogenous U2 snRNP and the pre-spliceosome (19). We observed similar levels of co-immunoprecipitation of radiolabeled U2 snRNA in the presence or absence of pre-mRNA, whereas previous studies found that co-precipitation of endogenous U2 is enhanced by added pre-mRNA (19). The lack of an enhancement of U2 binding by added pre-mRNA in the reconstitution protocol may be due to the use of very low levels of active U2 snRNA. Precipitation of the U2Δ107 RNA showed a similar pattern of binding compared with the full-length U2 but occurred at an overall reduced efficiency (*lanes 2, 5, 8,* and *11*).

The finding that antibodies to Prp21 and Prp11 immunoprecipitate U6 in a pre-mRNA-dependent manner indicate that Prp21 and Prp11 bind to a spliceosomal complex which is more mature than the pre-spliceosome. Although we did not have antibody to Prp9, our finding that Prp9, Prp11, and Prp21 form a highly stable complex under similar *in vitro* conditions suggests that Prp9, as part of the 9.11.21 complex, is also associated with a U6-containing spliceosomal complex.

Prp21 Is a Component of the A1 Complex—To identify specific spliceosomal complexes containing the Prp11 and Prp21 proteins, we performed immunodepletion experiments similar to those of Arenas and Abelson (19). The protocol involves incubation of splicing reactions with antibody beads followed by a brief centrifugation to pellet complexes to which the antibody has bound. A fraction of the supernatant is then loaded to a native polyacrylamide gel, and spliceosomal complexes formed with radiolabeled pre-mRNA are separated by electrophoresis. Complexes bound by antibody are identified by their absence from the native gel. In the immunodepletion experiment of Fig. 6, we included 2 mM EDTA in the splicing reaction. This results in inhibition of the formation of complexes beyond the A1 complex and leads to a build up of the A1 complex as well as prior intermediates (16) *Lane 1* shows complexes formed in an EDTA reaction not treated with antibodies or beads. The B complex (pre-spliceosome), A2-1, and A1 complexes are seen. As expected in the reaction treated with Prp21 antibody beads, there is quantitative removal of the B complex (*lane 2*). In addition, a portion of the A1 complex is removed. In reactions treated with beads only or buffer only all complexes remain in the supernatant (*lanes 3* and *4*). The finding that only part of the A1 complex was removed suggested that the A1 complex described on these native gels may be composed of two different species, migrating at or very close to the same position. To further characterize the precipitated complex, we repeated the immunodepletion experiment in heat-inactivated extracts from a *prp2-1* temperature-sensitive strain. We chose this mutant extract because the Prp2 protein has been shown

to act on the A1 complex.[2] *Lane 5* shows complexes formed in a heat-inactivated *prp2-1* extract. A small amount of B complex is formed as well as a complex migrating similar to the A1 complex in EDTA-treated wild type extracts. Visualization of the A2-1 complex in addition to the B and "A1" complex in inactivated *prp2-1* extracts requires inclusion of EDTA in the reaction (data not shown). When the *prp2-1* extract is treated with Prp21 antibody beads, virtually all the B and A1 complex is removed (*lane 6*). No complexes are removed when the reaction is treated with beads only or buffer only (*lane 7* and *8*). Taken together the quantitative binding of Prp21 antibodies to the A1 migrating complex formed in the *prp2-1* mutant extract and the binding to a portion of the A1 complex in the EDTA-treated wild type reaction suggest that the A1 complex in the wild type extract is composed of two different complexes. The upper complex with reduced mobility is dependent on the action of the Prp2 protein and is not immunodepleted by antibodies to Prp21. Thus Prp21 is a component of an A1 complex.

Because Prp11 antibodies also immunoprecipitated a U6-containing complex, we attempted to perform the spliceosome complex immunodepletion experiments with the Prp11 antibodies described in Fig. 5. We were unable to see immunodepletion of even the pre-spliceosome complex. This inability to immunodeplete with Prp11 antibodies may be due to differences in reaction conditions for the immunodepletion of complexes and the immunoprecipitations described above (*i.e.* the presence or absence of heparin in the reactions). However, based on the immunoprecipitation of U6, Prp11 is very likely also a component of the A1 and/or another spliceosomal complex.

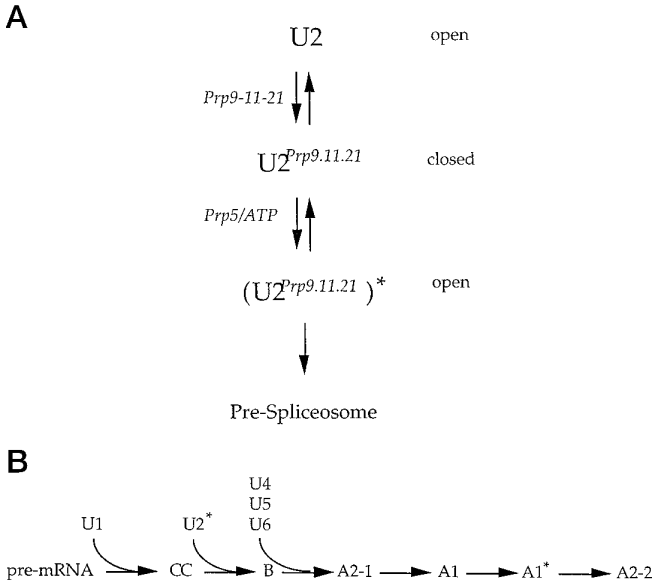

FIG. 7. **U2 snRNP activation and spliceosome assembly.** *A*, schematic diagram of the proposed model for Prp5-, Prp9-, Prp11-, and Prp21-dependent structural changes in the U2 snRNP. *B*, diagram of the spliceosomal assembly pathway.

DISCUSSION

There are several lines of evidence to suggest that Prp9, Prp11, and Prp21 interact with each other to form a protein complex. First, SF3A, the mammalian splicing factor consisting of the Prp9, Prp11, and Prp21 homologs (SAP61, SAP62, and SAP114, respectively) (28–31), behaves as a tight protein complex *in vitro* when subjected to extensive column chromatography (32). In addition, far Western type experiments testing SAP61 and SAP62 with SAP114 showed a direct interaction between these components of SF3A (28, 33). Second, genetic analysis of yeast strains carrying any two of the temperature-sensitive mutations of the *prp9-1*, *prp11-1*, or *prp21-1* alleles exhibited a synthetic lethal phenotype, suggesting a tightly coupled role for these proteins (16, 17). Finally, two-hybrid experiments performed with the coding regions of Prp9, Prp11, and Prp21 revealed that these proteins interact *in vivo* in a manner consistent with the formation of a Prp9·Prp11·Prp21 complex (22, 23).

Although these lines of evidence are compelling, there had been no biochemical investigation of the yeast Prp9·Prp11·Prp21 complex. We have presented here direct physical evidence for the yeast Prp9·Prp11·Prp21 complex and have begun to characterize the biochemistry of this complex *in vitro*. First, we demonstrated a direct interaction between Prp11 and Prp9 and Prp21 by demonstrating that the entire complex is inactivated by heat in *prp11-1* or *prp21-1* extracts. All three proteins must be added to regain activity. The formation of a Prp9·Prp11·Prp21 complex in the absence of any other yeast proteins was studied by analyzing proteins made in a rabbit reticulocyte *in vitro* translation system. Prp9·Prp11·Prp21 formed *in vitro* is highly stable even at salt concentrations greater than 0.5 M NaCl. Interestingly, Legrain and colleagues (23) demonstrated formation of a Prp9 homodimer using the yeast two-hybrid assay system. We were unable to detect homodimers of either Prp9, Prp11, or Prp21 in our *in vitro* experimental system. It is possible that observation of homodimer formation by Prp9 requires an additional factor(s) not present in our *in vitro* system.

Previous genetic experiments also demonstrated synthetic lethal interactions of *prp9-1*, *prp11-1*, and *prp21-1* with *prp5-1* mutants (16, 17). We were unable to detect a direct interaction between Prp9·Prp11·Prp21 and Prp5, so we investigated the possibility that the observed genetic interaction between these proteins was mediated through a functional interaction. In the accompanying paper (18), we demonstrated that Prp5 mediated an ATP-dependent structural change in the U2 snRNP, leading to exposure of its branch point region. We hypothesized that this exposure of the branch point region facilitated interaction of the U2 snRNP with the complementary region of the pre-mRNA. In this paper, we demonstrated that Prp9·Prp11·Prp21 is necessary for stabilization of a U2 structure that Prp5 can utilize as a substrate.

Based on differences in RNaseH sensitivity of U2 RNA in mutant extracts, we propose a model in Fig. 7 for changes in U2 snRNP conformation in the activation of the U2 snRNP during spliceosome assembly. This model describes two "open" (RNaseH-accessible) states. These two states are differentiated by whether or not they require ATP to form and by their ability to assemble into a pre-spliceosome. In the absence of ATP, there are two (or more) conformational states that are in dynamic equilibrium. The open form of the equilibrium is inactive in pre-spliceosome assembly. In the absence of Prp9, Prp11, and Prp21 (*e.g.* in a heat-treated *prp9-1* extract), this equilibrium favors the inactive, open state. Addition of Prp9·Prp11·Prp21 in the absence of ATP favors a shift to the closed state. In the presence of ATP and *PRP5* this closed complex is transformed to an active open state poised for interaction with the branch point sequence of the pre-mRNA.

Ares and colleagues (9, 10) have shown that in the U2 cold-sensitive mutants G53A and C62U, the U2 snRNA favors an altered secondary structure or misfolded form that is in equilibrium with competent snRNP (9, 10). These mutants are synthetically lethal with *prp5-1*, *prp9-1*, *prp11-1*, and *prp21-1* (16, 17). Our investigation of the U2 snRNP in these mutant extracts indicated that virtually all of the snRNP was in an

[2] R.-J. Lin, personal communication.

open conformation even in the absence of ATP. Thus the synthetic lethality could be explained by the lack of a significant population of Prp9·Prp11·Prp21-associated U2 snRNP for Prp5 to activate. The G53A and C62U mutations affect the equilibrium between different forms of the stem II structure of U2 RNA. It is not clear how different forms of this structure could affect the accessibility of the branch point interaction sequence; however, recent work by Yan and Ares (34) has identified U2 mutants very close to the branch point pairing sequence that interact synergistically with mutants in *PRP5, PRP9, PRP11,* and *PRP21.* The mutants are changes in U40, C41, U45, C46, and U47 just downstream from the branch point interaction sequence between residues 34 and 39. How changes in the 40–47 region affect U2 function is not clear, but one possibility is that the mutants enhance pairing with a sequence in U2 between 25 and 30. Such a helical interaction might prevent the pairing between U2 and the intron. It will be very interesting to find out how mutants in the 40–47 region score in the RNase H assay.

Other members of the DEAD family of RNA helicases show characteristic low binding affinities for their RNA substrates (35, 36). Although the detailed mechanism for specific RNA-dependent ATP hydrolysis and RNA unwinding by these proteins is not well understood, a possible mechanism could be the use of auxiliary proteins to facilitate activity and/or specificity. In the case of eIF-4A, eIF-4B is necessary to stimulate helicase activity (37). eIF-4B contains an RNP motif suggestive of an RNA binding function (38). Thus, a possible role for eIF-4B may be to stabilize or enhance RNA structures suitable for use as substrate by eIF-4A. Analogously, it has been shown that Prp9·Prp11·Prp21 binds to the U2 snRNP (27) and stabilizes the RNaseH inaccessible ("closed") form of the U2 snRNP that is a substrate for Prp5 (this work). The availability of purified Prp9·Prp11·Prp21 protein complex should greatly facilitate investigation of potential Prp5 RNA helicase activity *in vitro*.

A Role for Prp9·Prp11·Prp21 after Pre-spliceosome Assembly—We have described convincing evidence that Prp9·Prp11·Prp21 associates with U2 and ultimately with the pre-spliceosome. Identifying possible roles of these proteins later in the spliceosome assembly pathway has been more difficult. Using a highly sensitive snRNA immunoprecipitation protocol based on the U6 knock out/reconstitution system (19), we have detected the presence of Prp9·Prp11·Prp21 in U6 snRNA containing spliceosomal complexes. Although we only directly detected co-immunoprecipitation of U6 with antibodies to Prp11 and Prp21, we favor the hypothesis that interactions detected with any one of the components of Prp9·Prp11·Prp21 represent the presence of the complex. This is because Prp9·Prp11·Prp21 is a highly stable complex under the *in vitro* conditions of the splicing assay. However, we cannot rule out the possibility that the complex is disrupted during spliceosome assembly. A diagram of the spliceosome assembly pathway is shown in Fig. 7*B*. We found that Prp21 could be identified as an integral component of an A1 complex. In earlier experiments (18) we did not detect a decrease in the U6-containing complexes in a Prp21 immune depletion experiment. This was probably because only part of complex A1 is depleted in these experiments, and the fraction that is in that form may depend on the experimental conditions. We were unable to detect Prp9·Prp11·Prp21 in the other U6-containing complexes, A2-1 and A2-2. It seems unlikely that Prp9·Prp11·Prp21 leaves the complex and returns at the later A1 stage, so we attribute the failure to deplete to conformational differences in these complexes leading to destabilization of Prp9·Prp11·Prp21 or to conformational differences that lead to inaccessibility of the epitope for immunoprecipitation.

Acknowledgment—We thank Jaime Arenas for providing the Prp21 expression plasmids.

REFERENCES

1. Green, M. R. (1991) *Annu. Rev. Cell Biol.* **7,** 559–599
2. Moore, M. J., Query, C. C., and Sharp, P. A. (1993) *The RNA World*, pp. 303–357, Cold Spring Harbor Laboratory, Cold Spring Harbor, NY
3. Madhani, H. D., and Guthrie, C. (1994) *Annu. Rev. Genet.* **28,** 677–687
4. Vijayraghavan, U., Company, M., and Abelson, J. (1989) *Genes Dev.* **3,** 1206–1216
5. Ruby, S. W., and Abelson, J. (1991) *Trends Genet.* **7,** 79–85
6. Guthrie, C., and Patterson, B. (1988) *Annu. Rev. Genet.* **22,** 387–419
7. Ares, M., Jr., and Igel, A. H. (1990) *Genes Dev.* **4,** 2132–2145
8. Miraglia, L., Seiwert, S., Igel, A. H., and Ares, M. (1991) *Proc. Natl. Acad. Sci. U. S. A.* **88,** 7061–7065
9. Zavanelli, M. I., and Ares, M. (1991) *Genes Dev.* **5,** 2521–2533
10. Zavanelli, M. I., Britton, J. S., Igel, A. H., and Ares, M. (1994) *Mol. Cell. Biol.* **14,** 1689–1697
11. Hodges, P. E., and Beggs, J. D. (1994) *Curr. Biol.* **4,** 264–267
12. Dalbadie-McFarland, G., and Abelson, J. (1990) *Proc. Natl. Acad. Sci. U. S. A.* **87,** 4236–4240
13. Legrain, P., and Choulika, A. (1990) *EMBO J.* **9,** 2775–2781
14. Chang, T.-W., Clark, M. W., Lustig, A. J., Cusick, M. E., and Abelson, J. (1988) *Mol. Cell. Biol.* **8,** 2379–2393
15. Chou, T.-B., Zachar, Z., and Bingham, P. M. (1987) *EMBO J.* **6,** 4095–4104
16. Ruby, S. W., Cheng, T.-W., and Abelson, J. (1993) *Genes Dev.* **7,** 1909–1925
17. Wells, S. E., and Ares, M. (1994) *Mol. Cell. Biol.* **14,** 6337–6349
18. O'Day, C. L., Dalbadie-McFarland, G., and Abelson, J. (1996) *J. Biol. Chem.* **271,** 33261–33267
19. Arenas, J. E., and Abelson, J. (1993) *Proc. Natl. Acad. Sci. U. S. A.* **90,** 6771–6775
20. Lin, R.-J., Newman, A. J., Cheng, S.-C., and Abelson, J. (1985) *J. Biol. Chem.* **260,** 14780–14792
21. Fabrizio, P., McPheeters, D. S., and Abelson, J. (1989) *Genes Dev.* **3,** 2137–2150
22. McPheeters, D. S., Fabrizio, P., and Abelson, J. (1989) *Genes Dev.* **3,** 2124–2136
23. Legrain, P., Chapon, C., and Galisson, F. (1993) *Genes Dev.* **7,** 1390–1399
24. Legrain, P., and Chapon, C. (1993) *Science* **262,** 108–110
25. Staknis, D., and Reed, R. (1994) *Mol. Cell. Biol.* **14,** 2994–3005
26. Bennett, M., Michaud, S., Kingston, J., and Reed, R. (1992) *Genes Dev.* **6,** 1986–2000
27. Abovich, N., Legrain, P., and Rosbash, M. (1990) *Mol. Cell. Biol.* **10,** 6417–6425
28. Bennett, M., and Reed, R. (1993) *Science* **262,** 105–108
29. Brosi, R., Groning, K., Behrens, S.-E., Luhrmann, R., and Kramer, A. (1993) *Science* **262,** 102–105
30. Behrens, S.-E., Galisson, F., Legrain, P., and Luhrmann, R. (1993) *Proc. Natl. Acad. Sci. U. S. A.* **90,** 8229–8233
31. Kramer, A., Legrain, P., Mulhauser, F., Groning, K., Brosi, R., and Bilbe, G. (1994) *Nucleic Acids Res.* **22,** 5223–5228
32. Brosi, R., Hauri, H.-P., and Kramer, A. (1993) *J. Biol. Chem.* **268,** 17640–17646
33. Chiara, M. D., Champion-Arnaud, P., Buvoli, M., Nadel-Ginard, B., and Reed, R. (1994) *Proc. Natl. Acad. Sci. U. S. A.* **91,** 6403–6407
34. Yan, D., and Ares, M. (1996) *Mol. Cell. Biol.* **16,** 818–828
35. Goss, D. (1987) *Biochemistry* **26,** 1551–1556
36. Abramson, R. D., Dever, T. E., and Merrick, W. C. (1988) *J. Biol. Chem.* **263,** 6016–6019
37. Ray, B. K., Lawson, T. G., Kramer, J. C., Cladaras, M. H., Grifo, J. A., Abramson, R. D., Merrick, W. C., and Thach, R. E. (1985) *J. Biol. Chem.* **260,** 7651–7658
38. Milburn, S. C., Hershey, J. W. B., Davies, M. V., Kelleher, K., and Kaufman, R. (1990) *EMBO J.* **9,** 2783–2790